Neuropsychologia 162 (2021) 108053

Contents lists available at ScienceDirect

Neuropsychologia

journal homepage: www.elsevier.com/locate/neuropsychologia

The form of reference frames in vision: The case of intermediate shape-centered representations

G. Vannuscorps [a,b,c,d,*], A. Galaburda [e], A. Caramazza [a,f]

[a] Department of Psychology, Harvard University, Cambridge, MA, 02138, USA
[b] Institute of Psychological Sciences, Université Catholique de Louvain, 1348, Belgium
[c] Institute of Neuroscience, Université Catholique de Louvain, 1348, Belgium
[d] Louvain Bionics, Université Catholique de Louvain, 1348, Belgium
[e] Department of Neurology, Harvard Medical School and Beth Israel Deaconess Medical Center, Boston, MA, 02215, USA
[f] Center for Mind/Brain Sciences (CIMeC), Università Degli Studi di Trento, Rovereto, 38068, Italy

ARTICLE INFO

Keywords:
Mid-level vision
Reference frame
Shape-centered representations

ABSTRACT

Although a great deal is known about the early sensory and the later, perceptual, stages of visual processing, far less is known about the nature of intermediate representational units and reference frames. Progress in understanding intermediate levels of representations in vision is hindered by the complexity of interactions among multiple levels of representation in the visual system, making it difficult to isolate and study the nature of each particular level. Nature occasionally provides the opportunity to peer inside complex systems by isolating components of a system through accidental damage or genetic modification of neural components. We have recently reported the case of a young woman who perceives 2D bounded regions of space as if they were plane-rotated by 90, 180 or 270° around their center, mirrored across their own axes, or both. This suggested that an intermediate stage of processing consists in representing mutually exclusive 2D bounded regions extracted from the retinal image in their own "shape-centered" perceptual frame. We proposed to refer to this level of representation as "intermediate shape-centered representation" (ISCR). Here, we used Davida's pattern of errors across 9 experiments as a tool for specifying in greater detail the geometrical properties of the reference frame in which elongated and/or symmetrical shapes are represented at the level of the ISCR. The nature of Davida's errors in these experiments suggests that ISCRs are represented in reference frames composed of orthogonal axes aligned with and centered on the most elongated segment of elongated shapes and, for symmetrical shapes deprived of a straight segment, aligned with their axis of symmetry, and centered on their centroid.

1. Introduction

Visual perception begins with a dynamic projection of the visual scene on the 2-dimensional layer of photoreceptors of our two retinas and culminates in a conscious experience of stable objects in a three-dimensional environment. A keystone in thinking about how this transformation operates is that it involves successive stages that progressively aggregate elementary features into more complex representations. A major goal of vision science is to characterize the form that mental representations take along these stages. This implies specifying two main aspects of these representations. The first is the "representational content", the nature of "what" is represented at any given stage. The second is the reference frame with respect to which this content is represented. Put simply, a reference frame is a means of representing spatially organized information, such as the arrangement of more elementary units into larger units (e.g., primitives into chunks of primitives, and, progressively, into shapes and objects). In vision research, reference frames are typically assumed to be a mental equivalent of a coordinate system composed of orthogonal axes (Marr and Nishihara, 1978; McCloskey et al., 2006; Palmer, 1999). Thus, characterizing the form of a reference frame implies specifying where it is centered (its origin) and how it is oriented.

A great deal is known about the form of the representations that characterize the early sensory and the later, perceptual, stages of visual processing. Previous research has established that vision starts with a representation of some type(s) of visual primitive(s) such as lines and edges (Hubel and Wiesel, 1968), blobs and terminators (Marr, 1982) and spatial frequency patches (De Valois and De Valois, 1988) in a

* Corresponding author. Institute of Psychological Sciences, Université catholique de Louvain, Place Cardinal Mercier, 10, Louvain-la-Neuve, Belgium.
E-mail address: gilles.vannuscorps@uclouvain.be (G. Vannuscorps).

https://doi.org/10.1016/j.neuropsychologia.2021.108053
Received 13 April 2021; Received in revised form 10 August 2021; Accepted 1 October 2021
Available online 5 October 2021

two-dimensional reference frame centered on the observer's fovea and aligned with the vertical and horizontal meridians of the eye, i.e., a retinocentric frame (Wandell et al., 2007). Accordingly, lesions to the first stages of cortical processing typically lead to a visual defect limited to information initially captured by photoreceptors located on one side of the vertical meridian, to a particular quadrant, or even a smaller area (scotoma) of the retina (Horton & Hoyt, 1991a, 1991b; McFadzean and Hadley, 1997).

At later stages, objects (cars, dogs, cups) appear to be represented with respect to various non-retinocentric reference frames. One primary source of evidence in support of the existence of these different reference frames comes from neuropsychological single-case studies. Brain-damaged patients have been reported who struggle to attend to, explore, and respond to visual information in a functional space located on one side of their body, of their head and/or eye midline (Beschin et al., 1997; Bisiach et al., 1985; Hillis et al., 1998; Karnath et al., 1991; Ladavas, 1987), one side of some environmental midline (Baylis et al., 2004; Calvanio et al., 1987) or on one side of an object separated in two by either environmental (Farah et al., 1990; Hillis and Caramazza, 1995; Tipper and Behrmann, 1996) or object-based axes (Driver et al., 1994). Such deficits would be difficult to explain without assuming that the brain ends up representing objects in various object-centered, body-centered, and environment-centered reference frames. The existence of these reference frames has been corroborated by behavioral and neuroimaging studies (Colby, 1998; Melcher and Morrone, 2015; Mullette-Gillman et al., 2005; Olson, 2003; Rock and Brosgole, 1964).

Beyond the intrinsic interest of this fundamental research, these findings have played an important role in the development of new technologies, such as biologically inspired artificial neural networks (ANNs) designed to recognize objects (e.g., Yamins et al., 2014; Pospisil et al., 2018). They have also improved our understanding of numerous visual disorders, from the nature of scotomas to that of different types of neglect and optic ataxia (Driver et al., 1994; Baylis et al., 2004; Hillis et al., 1998; McFadzean and Hadley, 1997). However, and although some work on shape coding in V4 has begun to explore these issues (El-Shamayleh and Pasupathy, 2016; Pasupathy and Connor, 2001), further progress in these directions is hampered by the fact that we still know very little about the nature of representational units and reference frames at intermediate stages of processing.

According to surface-based models of shape representation, an intermediate level of representation consists in representing mutually exclusive 2D bounded regions extracted from the retinal image by edge detection mechanisms operating on different sources, such as color, luminance, texture, motion and binocular disparity (Leek et al., 2005; Marr, 1982; Palmer and Rock, 1994). And indeed, there is evidence that 2D bounded regions are computed at some stage of processing (Arguin et al., 2019; Barton et al., 2007; Leek et al., 2005; Palmer and Rock, 1994). For instance, brain-damaged patients suffering from "object-based" simultanagnosia who typically behave as if they could see only one shape at a time, can perceive multiple shapes (e.g., three pacmen) when they are connected by a thin line (Barton et al., 2007). However, empirical data relevant to characterizing the functional locus of these representations and the nature of their associated reference frame are largely lacking.

Progress in this direction is hindered by the difficulty to experimentally isolate and study intermediate, unconscious, stage of processing. However, nature occasionally affects the functioning of an isolated, unconscious, intermediate stage of processing and thereby provides an unparalleled opportunity to deduce its representational and computational nature (e.g., Caramazza and Hillis, 1990; Schubert and McCloskey, 2013). We have recently reported the study of a young woman, Davida, who presented with a specific visual disorder that provided strong support for, and new insights about, intermediate edge-bounded 2D shape representations (see Vannuscorps et al., 2020 for a complete report). Davida's results in more than 80 experiments probing her perception through verbal judgments, visual illusions, copying, and directed movements indicated that she perceives each 2D region of space bounded by sharp chromatic or luminance edges (e.g., black or colored letters, arrows, abstract shapes on white background) alternating piecemeal between their correct orientation and all the other orientations that would result from their mirroring across their own axes, their rotation by 90, 180 or 270° around their center, or both (see Fig. 1). For instance, when shown a tilted elongated asymmetrical shape like that shown in Fig. 1a and asked to report all the orientations of that shape that she perceives, Davida reports seeing that shape in the 8 orientations shown in Fig. 1 (Vannuscorps et al., 2020; Experiment 4.3). Among these multiple percepts, Davida is entirely unable to discriminate the one corresponding to the correct orientation of the stimulus from those corresponding to rotations and/or reflection of that stimulus. Hence, when shown a shape like that shown in Fig. 1a and asked to report the most likely orientation of that shape among those that she perceives, Davida reports seeing the same 8 orientations in varying proportions (Vannuscorps et al., 2020; Experiment 4.1). In contrast, she is as good as control participants in judging the shape, size, location, distance, tilt, and movement of 2D stimuli, and her perception of the orientation of 3D shapes and of strongly blurred or very low contrast 2D shapes is intact.

The finding that Davida's disorder affected specifically the perception of 2D regions of space bounded by sharp chromatic or luminance edges constitutes proof that, at some stage of processing, the visual system represents 2D bounded regions, independently from context. Indeed, the similarity between the perceptual units affected by Davida's disorder and those assumed to be computed at an intermediate stage of processing in some surface-based theories is striking (Leek et al., 2005; Palmer and Rock, 1994). According to Palmer and Rock (1994), for instance, intermediate representations of 2D bounded regions emerge from edge detectors that are selectively sensitive to sharp spatial changes in a given visual property (e.g., luminance). This predicts that two regions of the retina divided by an abrupt change of some visual property (e.g., abrupt change of luminance) should result in two distinct representations, but that two regions separated by a slowly changing transition (e.g., gradual change in luminance) should result in a single representation. In line with this hypothesis, we found that Davida perceives a bicolor shape as two separate misoriented bounded regions when the two colors are separated by a sharp edge, but as one single misoriented perceptual unit when the two colors are progressively blended into each other (Experiment 5.6 in Vannuscorps et al., 2020; see also Movie S14 on osf.io/sp6cz/?view_only=fe6e9e7d30bb4b2bbb3f403bd2ff99f9).

Davida's disorder also provided new information about the functional locus of this stage of representation. Surface-based representations are often assumed to be an intermediate step in the process of object recognition (Hummel, 2001; Marr, 1982; Marr and Nishihara, 1978). The fact that Davida's disorder affected similarly her performance in all tasks, including pointing and grasping tasks, suggested that this intermediate stage of representation is preliminary to the functional specialization of the visual system into subsystems involved in perception and action. This is in line with Palmer and Rock's (1994) hypothesis that 2D bounded regions are computed at an early stage of processing, bridging edge detection and figure/ground segmentation.

Another feature of Palmer and Rock (1994)'s hypothesis supported by the nature of Davida's disorder is the idea that multiple 2D bounded regions are computed in parallel by edge detection mechanisms operating on different visual information, such as color, luminance, texture, motion and binocular disparity. According to this hypothesis, a single region of the retina (e.g., a red triangle on white background) bounded by edges that can be captured by different types of detectors (e.g., both color and luminance) will be represented twice – once in a map resulting from the detection of the changes in luminance and another from the detection of the chromatic change. That Davida's disorder affects the perception of the orientation of 2D regions bounded by some types of edges (sharp luminance and chromatic edges), but not others (disparity,

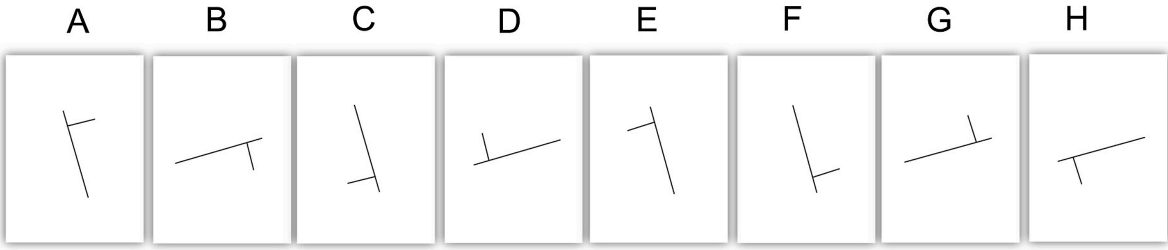

Fig. 1. Illustration of Davida's types of errors for a tilted asymmetrical shape (A). Davida systematically made the same 7 types of errors: she perceived the shape as if it were rotated by 90 (B), 180 (C) or 270 (D) degrees around its center, as if it were reflected across its elongation axis (E), as if it were rotated across a perpendicular to its elongation axis by its center (F), or combinations of both types of errors (G, H).

motion cues and edges defined by a very low luminance contrast with the background) is in line with this idea. In this framework, Davida's profile can be explained as a deficit occurring during the mapping of intermediate shape representations computed from some visual cues (sharp luminance and/or chromatic edges) onto a higher (e.g., spatiotopic, body-centered) frame (see Vannuscorps et al., 2020; see also McCloskey et al., 2006 for a detailed discussion of the theoretical framework for the interpretation of orientation errors).

Finally, and more importantly for the purpose of the study reported herein, the nature of Davida's pattern of errors provided a window into the reference frame in which information is organized at that stage of processing. Two main aspects of Davida's profile are of particular relevance here. The first is that the nature of Davida's errors (e.g., the specific types of rotation and reflection errors) was independent of the location of the stimulus in her visual field, on the screen, of where she focuses her attention (on the stimulus or not), of the presence of other stimuli in the environment, and of the orientation of her head, of her body or of the computer screen. This allowed us to conclude that her disorder is that of seeing shapes rotated (and reflected) around their own center, not around her fovea, the center of the screen or her attentional focus. This conclusion was corroborated by the observation that, when presented simultaneously with two shapes, even for a very short duration (32 ms), Davida perceived both as if they were rotated or reflected with respect to their own center. The second aspect is that Davida perceives tilted elongated stimuli as if they were rotated "with respect to themselves" (Fig. 1B–D), reflected across their elongation axis (Fig. 1E), reflected across an axis perpendicular to the elongation axis (Fig. 1F), or as if their orientation resulted from a combination of these transformations (Fig. 1G and H). Tilted stimuli allow disentangling shape-based axes (e.g., the elongation axis of elongated stimuli) from axes aligned with the observer's own midline or on scene-based "vertical" axes. Hence, this profile of errors implies that her disorder is of perceiving shapes reflected across axes aligned with the shape itself. Under the assumption that the center and axes revealed by her rotation and reflection errors, respectively, reveal the center and axes of the shape's reference frame, these errors indicated that elongated 2D bounded regions are represented in a reference frame centered on the center of the shape and composed of an axis aligned with the shape's elongation axis. For this reason, we proposed to refer to this level of representation as "intermediate shape-centered representation" (ISCR; Vannuscorps et al., 2020).

However, these previous results provided only incomplete evidence about the geometrical properties determining the center (origin) and orientation of the reference frame at the stage of ISCR. One limitation of our conclusion is that we did not formally define what actually constitutes the "elongation" axis and the "center" of elongated shapes. As noted by Chaisilprungraung et al. (2019), three definitions of what constitutes an elongation axis should be distinguished: (a) an axis aligned with the longest segment of an elongated shape (Chaisilprungraung et al., 2019; Driver and Halligan, 1991; McCloskey et al., 2006); (b) an axis relating the two most distant points of the shape (longest span axis; Sekuler and Swimmer, 2000); (c) an axis that minimizes the sum of squared distances to all points of the shape (the axis of least second moment; Cohen and Singh, 2006; Cheng, 2005). The nature of Davida's reflection errors in previous experiments with tilted elongated stimuli (e.g., Fig. 1E) suggested that her errors are reflections across an axis aligned with the longest segment of an elongated shape but this possibility was never directly contrasted with the two others. The goal of Experiment 1, reported below, was to discriminate these possibilities in order to determine the heuristics used by the visual system to orient reference frames in which ISCRs of elongated shapes are represented.

Likewise, Davida's errors in previous experiments did not allow for deciding whether the center of the reference frame of elongated shapes is ascribed to the shape's centroid (mean coordinate of all the points in the shape; Ayzenberg and Lourenco, 2019; Cheng, 2005; Palmer, 1999) or to the center of the shape's longest segment (McCloskey et al., 2006). One reason is that we used mostly stimuli whose centroid was overlapping with, or lied very close to, the center of the longest segment of the shape, making it difficult to discriminate errors resulting from rotations around one from the other. A second reason is that our previous experiments were not designed for this purpose and did not allow us to collect data of sufficient precision to discriminate these two possibilities. The goal of Experiments 2 and 3, reported below, was to overcome these limitations and explore whether Davida's rotation and reflection errors emerge in a reference frame centered on the centroid or on the center of the longest segment of elongated shapes. Here again, the goal was to exploit these data to draw inferences about the geometrical property used by the visual system for defining the center of the internal reference frame of such ISCR.

A more general limitation of our previous findings is that they were limited to elongated asymmetrical shapes. Therefore, another objective of the set of experiments reported herein was to use Davida's errors to explore the form of reference frames, at the level of the ISCR, used by the visual system to represent symmetrical shapes deprived of a straight segment (Experiments 4–7) and symmetrical shapes composed of a straight segment (Experiments 8–9). It is often assumed that the visual system uses the axis of symmetry to represent symmetrical shapes (Palmer, 1985; Marr, 1982; Sekuler and Swimmer, 2000; Quinlan and Humphreys, 1993), but this remains to be empirically demonstrated at the stage of ISCRs. Furthermore, the location of the center of the reference frame remains to be specified and it is unclear whether the center of an axis of elongation or the shape's centroid is prioritized by the visual system when both are available.

2. Case report

Davida is a very cooperative right-handed (Oldfield's Laterality Index of 80) young woman, who has previously been reported to perceive sharp-edged, medium to high-contrast 2-dimensional (2D) stimuli (e.g., numbers and road signs) in a series of different orientations that alternate piecemeal through a gradual transition (Vannuscorps et al., 2020). This highly selective disorder contrasted with otherwise normal perception of the 3D environment under naturalistic viewing conditions, of the orientation of strongly blurred or very low contrast shapes, and of the shape, size, location, distance, tilt, and movement of 2D stimuli.

The origin of her deficit at the neural level is unknown. She has no remarkable medical history and her neurological examination (including electroencephalogram and structural magnetic resonance imaging) revealed a normal brain with no evidence of changes of volume or shape, cortical malformations or early injury. There were no issues to report in the psychiatric history. A neuropsychological evaluation that took place just before the study began revealed no deficit that could not be explained by her visual disorder. Hence, Davida displayed: (1) average or above average performance on all the subtests of the WISC-IV (Vaughn-Blount et al., 2011; all tests 37 < percentile <84); (2) typical verbal (percentile 34) and visual (percentile 27) memory on the Wide Range Assessment of Memory and Learning-2 (Sheslow and Adams, 2003); (3) no clinically relevant executive function deficits on the Behavior Rating Inventory of Executive Function (Gioia et al., 2000) (all Teacher's and Parents' T-scores < 65) or on the Tower test of the Delis-Kaplan Executive Function System (Delis et al., 2001) (Percentile 37); (4) no clinically relevant behavioral abnormalities on the Conners' 3-T rating scale (Conners, 2010), other than the presence of learning problems (Teacher's and Parents' T-scores > 80; all other scales Teacher's and Parents' T-scores < 55); (5) intact phonological awareness and meta-phonological skills on the CTOPP-2 (Wagner et al., 1999) (Phonological Awareness Index, Elision, Blending Words and Phoneme Isolation tests, all 16 < Percentile <92); (6) excellent reading comprehension (percentile 95th on the untimed Grey Diagnostic Reading Test (Bryant et al., 1991)), thus suggesting that, despite her lack of fluency, she was able to accurately extract meaning from text; (7) age-appropriate listening comprehension on the Understanding Spoken Paragraphs subtest of the CELF-5 (Wiig et al., 2003); and (8) strong abstract thinking skills on the D-KEFS 20 (Delis et al., 2001). In contrast, and as expected given the nature of her visual disorder, Davida displayed below average speed on rapid naming of letters, numbers (she was at Percentile 1 or below at the Rapid Letter and Rapid Digit Naming tests of the CTOPP-2) and words (she was at the percentile 1 for her age on the TOWRE-2 (Torgesen et al., 2012) and atypical performance on the Test of Variables of Attention (McCarney and Greenberg, 1990). An ophthalmological examination revealed no other anomaly than a rapidly alternating ocular suppression and, as a consequence, an absence of perception of 3-dimensional structure based on binocular integration. She was 15 years old when this study began in October 2016 and 17 years old when it ended in March 2019. Her perceptual disorder was stable during the duration of the study. A more detailed case report is available in Vannuscorps et al. (2020).

3. Experimental study

3.1. General method

The experimental investigations were carried out from October 2016 to March 2019 during sessions lasting between 60 and 120 min. The study was approved by the Committee on the Use of Human Subjects, Harvard University (Protocol # IRB16-1124). Written informed assent (Davida) and permission (Davida's parents) were obtained prior to the study. Unless otherwise indicated, in all experiments Davida sat in front of a laptop computer at about 50 cm from the screen. The room was dimly illuminated from the ceiling. All experiments were controlled with the Psychopy software (Peirce, 2007, 2009), and all visual stimuli were displayed on a Lenovo T460s 14 inch, 16:9, 1920 x 1080 pixels (157 PPI), 60 Hz screen controlled by an Intel® HD Graphic 520 graphics card. Supplementary Movies can be accessed on the Open Science Framework platform (link: https://osf.io/pq6yk/?view_only=69562bf51fcf4244880b6b9775407eac).

3.2. Experiments 1–3. The reference frame of asymmetrical elongated ISCRs

3.2.1. Experiment 1. the orientation of an asymmetrical elongated shape's reference frame

This experiment took advantage of two aspects of Davida's visual disorder (Vannuscorps et al., 2020): (1) she misperceives the orientation of shapes defined by medium-to-high luminance contrast but perceives accurately and without any difficulty the orientation of the same shapes defined by a very low luminance contrast with the background; (2) Davida perceives each shape defined by medium-to-high luminance contrast alternating between its correct orientation and all the types of errors illustrated on Fig. 1. This allowed us to ask Davida whether a shape shown at a very low luminance contrast (which she perceives accurately) corresponds to a perceived orientation of shape shown at high luminance contrast (which she perceives in several orientations).

A prerequisite to the experiment was to determine the level of luminance at which Davida could see the shape shown in the experiment, including its orientation, perfectly. To do this, we presented Davida with a shape identical to that used in the main experiment at a very low level of luminance (black) on white background and asked her to modify the luminance of the shape (decrease and increase by pressing on the left and right buttons of the computer mouse) until she could see it perfectly well. She reported seeing that shape perfectly well (its orientation was perfectly stable) at a very light grey level (RGB of 252). This value was highly consistent with her result in several previously reported experiments, showing that Davida's perception becomes normal at such very low levels of luminance contrast (Vannuscorps et al., 2020; Experiments 6.3–6.9).

In each of the 24 trials of this shape association task, Davida was shown a shape (target) and, below it, an array of three shapes (the probes) displayed at very low contrast (RGB values of 252) with respect to the white background (RGB values of 255). The long segment of the shapes subtended ±5 degrees of visual angle. The three probes were mirror reflections of the target across an axis aligned with either the shapes' most elongated part (Fig. 2 B), the axis of least second moment (Fig. 2 C), or the longest span axis (Fig. 2 D). In each trial, the position of these three types of probe (left, center and right) was assigned pseudorandomly. Across the 24 trials, the target was displayed twice as shown in Fig. 2 and twice in each of 11 rotations of that stimulus by steps of 30° (30, 60, 90, 120, 150, 180, 210, 240, 270, 300, 330). Davida's task was to point to the probe corresponding to one of the orientations of the perceived target or to press the space bar if none corresponded.

Davida pointed to the probe corresponding to a reflection of the target across its longest segment (Fig. 2 B) in 100% of the trials. This finding allowed the clear conclusion that her errors emerge at a stage of processing in which elongated shapes are represented in a reference frame composed of an axis aligned precisely on the shape's longest segment. This finding does not allow discriminating whether the center of the frame is determined by the center of the shape's longest segment (McCloskey et al., 2006) or by the shape's centroid (Ayzenberg and Lourenco, 2019; Cheng, 2005; Palmer, 1999), however (see Fig. 4). The next two experiments were designed to address this issue.

3.2.2. Experiment 2. the center of asymmetrical elongated shape's reference frame

This experiment aimed at discriminating whether the center of the reference frame of an elongated shape is the center of the shape's longest segment (red dot in Fig. 3A and B) or the shapes' centroid (green dot in Fig. 3A and B). For this, it relied on the fact that Davida almost systematically perceives asymmetrical elongated shapes alternating between percepts in which the longest segment of the shape is either accurately oriented (Fig. 1 C, E, F) or rotated by 90° (Fig. 1 B, D, G, H). Under the assumption that the percepts of the shape's longest segment when the shape is perceived in its accurate orientation and when the shape is perceived as rotated by 90° intersect at the level of the center of

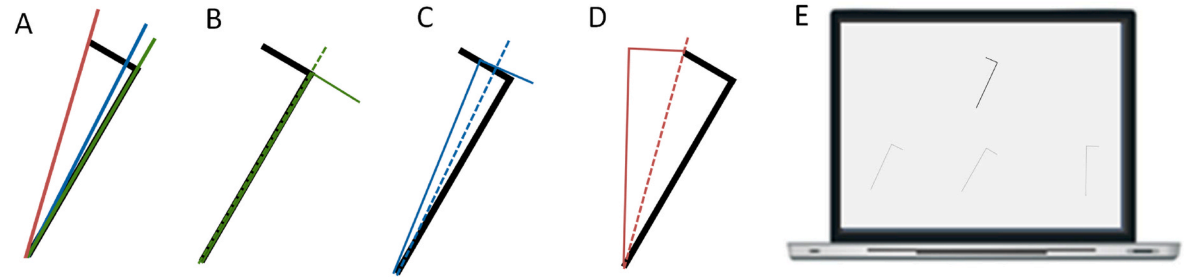

Fig. 2. A. Illustration of the shape's longest segment (green), longest span axis (red) and axis of least second moment (blue). B. Mirror reflection (in green) of the shape (in black) across an axis aligned with the shape's most elongated part. C. Mirror reflection (in blue) of the shape (in black) across an axis aligned with the shape's axis of least second moment. D. Mirror reflection (in red) of the shape (in black) across an axis aligned with the shape's longest span axis. E. Illustration of the experimental display. Top: the target. Bottom: mirror reflections of the target across an axis determined by the shape's longest straight segment (left), axis of least second moment (center) and longest span axis (right). The contrast of the probes was greatly increased in this example to make them more visible to the reader. (For interpretation of the references to color in this figure legend, the reader is referred to the Web version of this article.)

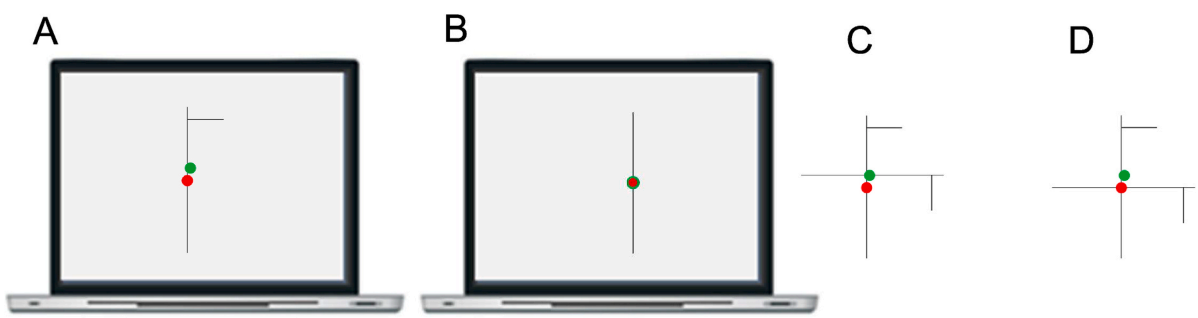

Fig. 3. A, B. Illustration of the stimuli used in Experiment 2 and of the position of the center of their longest part (the red dot) and of their centroid (the green dot). The center and centroid of the simple line being located at the same position, they are depicted as overlapping circles. C, D. Illustrations of possible percepts the center of these shapes' representational frames is defined by their centroid (C) or at the level of the center of their most elongated part (D). (For interpretation of the references to color in this figure legend, the reader is referred to the Web version of this article.)

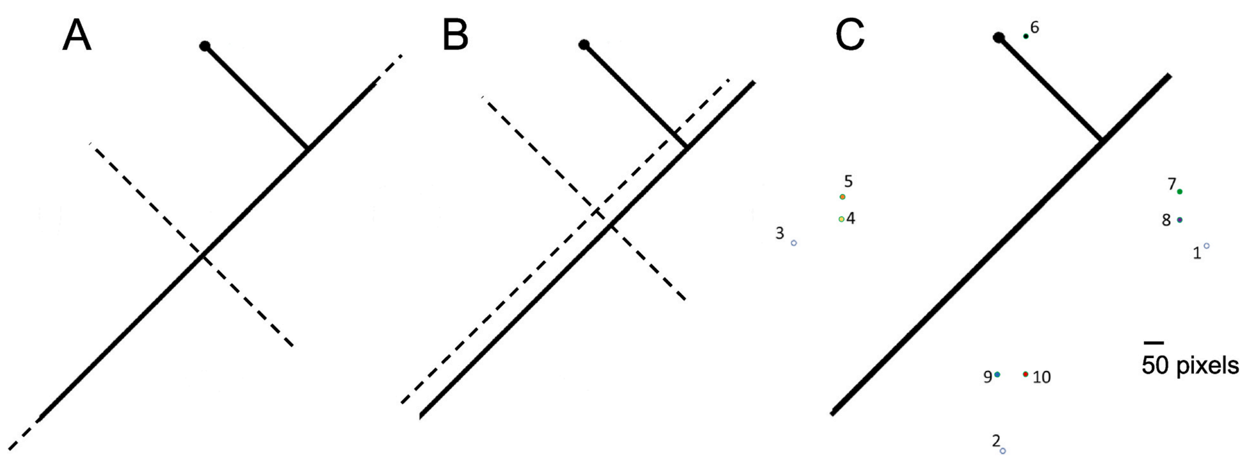

Fig. 4. A, B. Illustration of the stimuli used in Experiment 3 and of a reference frame centered on the longest segment of the shape (A) or on the shape's centroid (B). C. The numbered small circles illustrate the locations where the dot located at the end of the shortest segment would be after transformations of that shape in a reference frame centered on the shape's longest segment (small circles numbered 1–3) or on the shape's centroid (small circles numbered 4–10). The locations indexed by the circles numbers 1–3 correspond to where the dot would be if the shape were rotated by 90 (1), 180 (2) or 270 (3) degree around the center of the longest segment, reflected across an axis aligned with the shape's longest segment and intersecting the center of the longest segment (1), across a perpendicular axis intersecting the center of the longest segment (3), or a reflection across both axes (2). The locations indexed by the numbers 4–10 correspond to where the dot would be if the shape was rotated by 90, 180 or 270° around the centroid (7, 10, 4), reflected across an axis oriented in line with the shape's longest segment and passing through the shape's centroid (8), across a perpendicular axis passing through the centroid (5), a reflection across both axes (10) and locations resulting from combinations of these transformations (6, 9).

the frame, this allowed us to determine the location of the center of the reference frame by simply asking Davida to locate as precisely as possible the point where she sees the two percepts of longest segment of the shape intersecting, if there is any.

In each trial of this experiment, Davida was presented with either a tilted asymmetrical shape or a simple line corresponding to the shape's longest straight segment (Fig. 3A and B) and was asked to either use the computer mouse to move a small round cursor and click as precisely as possible on the place where she saw two lines crossing each other or to press the space bar if she did not see any line crossing. The shapes subtended ±8 degrees of visual angle. There was no time constraint. Each stimulus was displayed three times in 12 different orientations (0–330° by steps of 30°) for a total of 72 trials (2 stimuli x 12 orientations x 3 repetitions).

The inclusion of a simple line stimulus in the design provided an additional opportunity to test whether the center of the reference frame of an elongated shape is the center of the shape's longest segment or the shapes' centroid. The center of the simple line is the same as the center of the shape's longest segment (see the red dots on Fig. 3A and B). However, the centroid of the simple line is different from the centroid of the asymmetrical elongated shape (compare the location of the centroid, in green, of these two shapes on Fig. 3). Therefore, if the center of the reference frame of elongated shapes is the shape's centroid, then, Davida should perceive the long segment of both shapes intersecting at different locations. In contrast, if the center of elongated shapes' representational frame is defined by the center of the shapes' longest segment (the red dot in Fig. 3 A, D), then, Davida should perceive lines intersecting at the center of the shapes' longest segment (Fig. 3 D) and there should be no difference between where the two percepts of the simple line and of the asymmetrical stimuli intersect.

During the task, Davida never used the space bar to indicate that she did not see lines crossing. The coordinates at which she indicated seeing the two percepts of the line intersecting was on average at 14.3 pixels from the center/centroid of the line stimulus (±2 mm, SD = 2.6). For the elongated shape, she indicated seeing the two percepts of the longest segment intersecting on average at a point located 14.9 pixels (±2 mm, SD = 5.7) from the center of the elongated shape, but 43 pixels from where the lines would have crossed if the center of the frame were determined by the centroid of the elongated shape (±7 mm, SD = 13.3). The result of a paired sample *t*-test indicated that she located the intersection of the two percepts of the elongated shape significantly closer to the center of that shape than to where the lines would have crossed if the center of the frame were determined by the shapes' centroid ($t\ (35) = 15.3$, $p < 0.001$, $d = 2.55$). Additional analyses revealed a very similar profile when only the first 18 or only the last 18 items were considered in the analysis (first half: $t\ (17) = 8.89$; second half: $t\ (17) = 14.66$), suggesting that this response profile was reliable throughout the experiment. There was a difference of only 6 pixels on average (SD = 4.7) between the place where Davida perceived the two percepts of the simple line intersecting and the place where the asymmetrical stimuli intersected, which is well within the range of variability of her responses to several presentations of the same line (on average 14 pixels between the three repetitions) or asymmetrical elongated stimuli (on average 13 pixels between the three repetitions). The results of an independent samples *t*-test indicated that the location where she reported seeing the two percepts of the elongated shape intersecting did not differ significantly from the location where she reported seeing the two percepts of the simple line intersecting ($t\ (70) = 0.07$, $p > 0.9$). Additional analyses revealed a similar profile when only the first 18 or only the last 18 items were considered in the analysis (first half: $t\ (34) = 0.92$; second half: $t\ (34) = 0.6$), suggesting that this response profile was reliable throughout the experiment. These results demonstrate that the center of the elongated shapes' representational frame is defined by the center of their longest straight segment rather than by the shape's centroid.

3.2.3. Experiment 3. the center and orientation of asymmetrical elongated shape's reference frame

This experiment aimed at confirming the findings of Experiments 1 and 2 with a new type of task and measure. It is based on the finding that Davida systematically makes the same seven types of errors with this type of shape (See Fig. 1). This allows us to predict what the percept of a shape would be if these transformations (i.e., errors) occurred in a reference frame centered on the center of the longest segment of the shape (Fig. 4A) or on the shape's centroid (see Fig. 4B) and to compare these predictions to Davida's actual percepts.

In each of the trials of this task, Davida was shown a tilted asymmetrical shape (±10 × 3.2 degrees of visual angle; Fig. 4) and asked to use the computer mouse to move a small round cursor and click as precisely as possible on a dot located at the extremity of the short segment. The shape was presented until a response was obtained. There was no time constraint. The shape shown on Fig. 4 and a shape corresponding to its mirror reflection was presented in 8 different orientations (15, 75, 105, 165, 195, 255, 285, 345°). There were five trials per condition, for a total of 80 trials (2 stimuli x 8 orientations x 5 repetitions).

For each trial, we measured the distance between where Davida located the dot and where the dot would have been as a result of one of her seven typical types of errors under the assumption that the center of the frame is either the center of the shape's longest segment (locations 1–3 on Fig. 4C) or the shape's centroid (locations 4–10 on Fig. 4C). Davida clicked on, or very close to, the actual location of the dot in 3/80 trials. In the other trials, the coordinates of Davida's response were closer to where the dot would have been following one of her 7 types of errors occurring in a reference frame centered on the center of the shape's longest segment (circles numbered 1–3 on Fig. 4C) in 70/77 trials (average distance of 47 pixels, SD = 26; ±7.5 mm) and closer to where the dot would have been following one of her 7 types of errors occurring in a reference frame centered on the centroid (circles numbered 4–10 on Fig. 3C) in 7/77 trials (average distance of 71 pixels; ± 11.5 mm). In these 7 trials the location of Davida's response was typically also very close to a place where the dot would have been following a transformation of the shape in a reference frame centered on the center of the longest segment of the shape (average distance of 86 pixels; ± 14 mm). The results of a paired sample *t*-test indicated that her errors (77/80 trials) consisted in mislocating the dot significantly closer to where it would have been following one of her 7 types of errors occurring in a reference frame centered on the center of the shape's longest segment than on the shape's centroid (($t\ (76) = 9.1$, $p < 0.001$, $d = 1.03$). A very similar profile emerged when only the first 40 or only the last 40 items were considered in the analysis (first half: $t\ (36) = 6.3$; second half: $t\ (39) = 6.66$), suggesting that this response profile was reliable throughout the experiment.

3.3. Experiments 4–7. The reference frame of symmetrical ISCRs

In the series of experiments reported in this section, we presented Davida with symmetrical shapes devoid of a straight part (e.g., disks, semicircles and arcs) in order to gather data relevant to characterizing the center and orientation of the reference frame for this type of shape at the level of the ISCRs. The orientation of internal reference frames of symmetrical shapes is often assumed to be determined by their axis of symmetry (Palmer, 1985; Marr, 1982; Sekuler and Swimmer, 2000; Quinlan and Humphreys, 1993). However, whether the axis of symmetry is also used to determine the orientation of the reference frame at the level of the ISCRs remains an open question. It could be, for instance, that the visual system is not equipped to detect symmetry at the level of ISCRs. In this case, these shapes could be ascribed a reference frame oriented in line with the gravitational vertical, which has been shown to govern the orientation of reference frames in the absence of other organizational structure (Rock, 1983). Likewise, the principles that determine the center of the reference frame for this type of shapes is unknown. One possibility is that the center is located at the level of the shape's centroid. An alternative is that the center of the frame is located at the intersection of the shape and its axis of symmetry. Davida's profile of error in these experiments was clear cut: all of her errors could be interpreted as the result of a 90, 180 or 270° rotation around the shape's centroid and/or a reflection of the shape across an axis aligned with the shape's axis of symmetry and/or a perpendicular axis intersecting it precisely at the shape's centroid. This suggests that, at the level of the

ISCRs, symmetrical shapes devoid of a straight part are represented in a reference frame composed of orthogonal axes aligned with their axis of symmetry and centered on their centroid.

3.3.1. *Experiment 4. disks*

In each trial of this experiment Davida was shown a large black disk (640 x 640 pixels; 10.32 degrees of visual angle) with a small semi-circular indent of the same color as the background (see Fig. 5) for as long as needed, and she was asked to use the computer mouse to move a small round cursor and click as precisely as possible on the place "where she sees the indent". She then pressed the space bar to launch the next trial. She was free to click any number of times on the stimulus. The disk was displayed with the indent rotated either 10 (like on Fig. 5), 20, 30, 60, 70, 80, 150, 160, 170, 190, 200, 210, 240, 250, 260, 280, 290, 300, 330, 340 or 350° clockwise from the vertical midline. Davida acted on two or three stimuli at each orientation for a total of 47 stimuli (the task had to be aborted due to time constraint).

This type of stimulus afforded clear predictions about the number and type of Davida's errors that would result from the use of different reference frames. If the reference frame of these shapes is aligned with their axis of symmetry, then, Davida should locate the indent at only three erroneous locations corresponding to a rotation of the disk by 90, 180 or 270°. Indeed, under this assumption, a reflection of the shape across its axis of symmetry would not lead to detectable error and a reflection of the shape across its perpendicular or across both axes would be indistinguishable from a 180° rotation of the shape (See Fig. 5B for illustration). In contrast, if the reference frame is determined by any other feature of the shape, or aligned with Davida's body, or with the environment (e.g., aligned with the border of the screen, the gravitational vertical), then, we should detect Davida's typical 7 types of errors (Fig. 5C), and the location of Davida's reflection errors will provide insight into the orientation of the reference frame.

The Movie S1, online, is a recording of Davida performing this task and illustrates her response profile. Across trials, Davida reported seeing the indent at either two (1/47), three (35/47) or four (11/47) different locations on the screen, providing a total of 152 coordinates. As shown on Fig. 5D, among these responses, 47 (30.9%) consisted in localizing the indent at its' correct location (i.e., Davida clicked at less than 1 degree of visual angle, 62 pixels, of the center of the indent) and the other consisted mainly in localizing the indent erroneously at less than 1 degree of visual angle from where it would have been if the disk had been rotated by 90 (30 trials; 19.7%), 180 (41 trials; 26.9%) or 270 (25 trials; 16.4%) degrees. Among the 9 other errors, one error (0.6%) consisted in localizing the indent erroneously at less than 1 degree of visual angle from where it would have been if the disk had been reflected across a vertical axis passing by the center of the disk (Fig. 5B), and 8 (5.2%) errors were at a distance of more than 1 degree of visual angle from any interpretable landmark. The results therefore indicated the existence of a reference frame composed of the shape's axis of symmetry and it's perpendicular intersecting either at the center of the axis of symmetry or at the centroid of the shape. These two possible locations of the center of the reference frame were difficult to discriminate with the type of stimulus and measure used in this experiment because the center and centroid were very close to each other. Experiments 5–7 were designed to corroborate the findings from this experiment with new types of stimuli that should also provide clearer indication about the location of the center of the frame.

3.3.2. *Experiment 5. semicircles*

In this experiment, we presented Davida with 40 semicircles (see Fig. 6A) on a sheet of paper and asked her to trace the shape with ink. The semi-circles had a diameter of ±6 cm and were oriented 30, 60, 120, 150, 210, 240, 300 or 330°. There were 5 trials per orientation. Davida traced the displayed shape accurately (Fig. 6B) in 10% of the trials (4/40). In all but one other trial, she inked the sheet of paper as if the shape were rotated by 90 (9/40; Figs. 6C), 180 (15/40; Fig. 6D) or 270 (11/40; Fig. 6E) degrees around the shape's centroid (illustrated by the green dot in Fig. 6).

3.3.3. *Experiment 6. arcs*

This experiment aimed at confirming the finding from Experiment 5 with a new type of stimulus (arcs). In each of the 36 trials of this experiment Davida saw the arc of a circle (corresponding to ± 8.2 cm; Fig. 7) on a sheet of paper and asked her to trace the shape with ink. The arcs were oriented 15 (see Fig. 7), 45, 75, 105, 135, 165, 195, 225, 255, 285, 315, 345° clockwise from the vertical and there were 3 trials per orientation. Davida accurately traced the displayed shape in 2/36 trials (Fig. 7B). In the other trials, she inked the sheet of paper as if the shape were rotated by 90 (15/36; Fig. 7 aac), 180 (10/36; Fig. 7D) or 270 (9/36; Fig. 7E) degrees around the shape's centroid (illustrated by the green dot).

Across Experiments 5 and 6, 98.5% of Davida's errors (69/70) consisted in tracing semicircles and arcs as if they were rotated around their centroid. This finding indicates that Davida's errors emerge in a reference frame centered on the centroid of symmetrical shapes that are devoid of a straight part. In addition, these results suggest that these shapes are represented in a reference frame aligned with the axis of symmetry of these shapes. Indeed, as already noted above, the absence of detectable reflection errors in Experiment 5 and 6 would be expected only if these shapes are represented in a reference frame aligned with

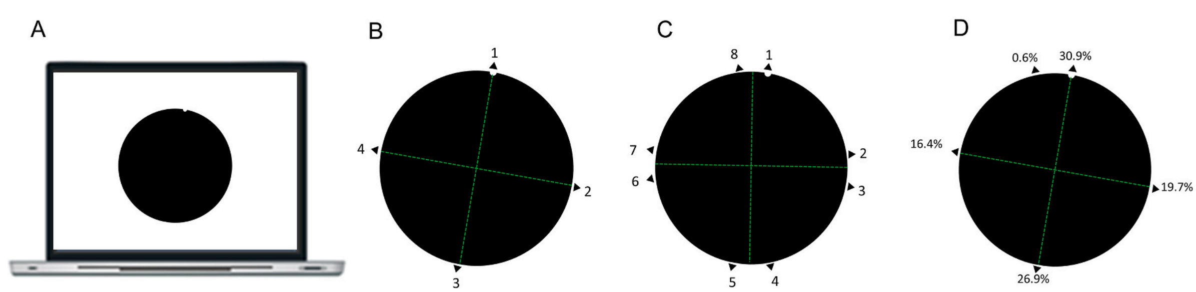

Fig. 5. A. Illustration of a stimulus used in Experiment 4 oriented 10° from the vertical clockwise. B. The green dotted lines illustrate a putative reference frame composed of an axis aligned with the disk's axis of symmetry, engendered by even a minimal deformation of a perfectly circular shape, and of its perpendicular passing through the shape's center. The numbered triangles refer to places where Davida would be expected to locate the indent if it were rotated by 90, 180 or 270° (2, 3 and 4, respectively), reflected across the shapes' axes (1 and 3) or combinations of these errors (2, 3, 4). C. The green dotted lines illustrate a putative reference frame composed of an axis aligned vertically and of its perpendicular passing through the shape's center. The numbered triangles refer to the places where Davida would be expected to locate the indent as a result of her typical 7 types of errors (see Fig. 1) emerging in this frame. Numbers 3, 5 and 7 correspond to 90, 180 or 270° rotations, number 8 to a reflection of the shape across a vertical axis, number 4 to a reflection of the shape across a horizontal axis, and number 2 and 6 correspond to combinations of rotation and reflection errors. D. The percentages refer to the proportion of Davida's responses corresponding to the different locations identified by the black triangles. The distribution of errors in this experiment clearly resulted from transformations of the stimulus within a reference frame aligned with the shape's axis of symmetry. (For interpretation of the references to color in this figure legend, the reader is referred to the Web version of this article.)

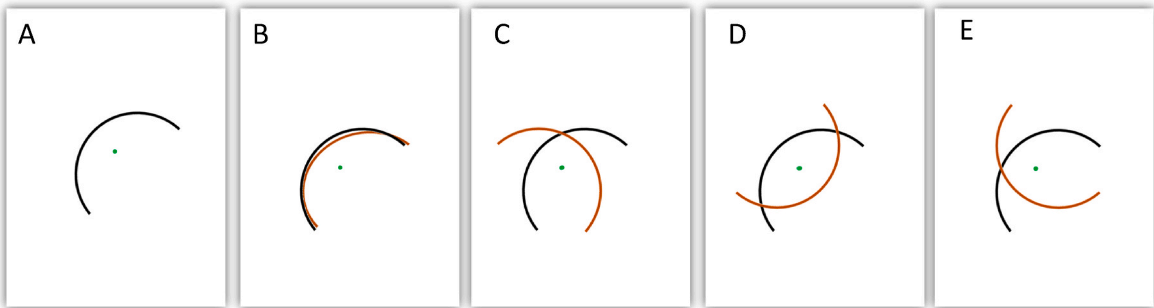

Fig. 6. A – E. Illustration of a semicircle stimulus used in Experiment 5 (A), of its' centroid (green dot), which was not shown during the experiment and of Davida's different types of responses when asked to trace the depicted shape with ink (B-E, in red ink). (For interpretation of the references to color in this figure legend, the reader is referred to the Web version of this article.)

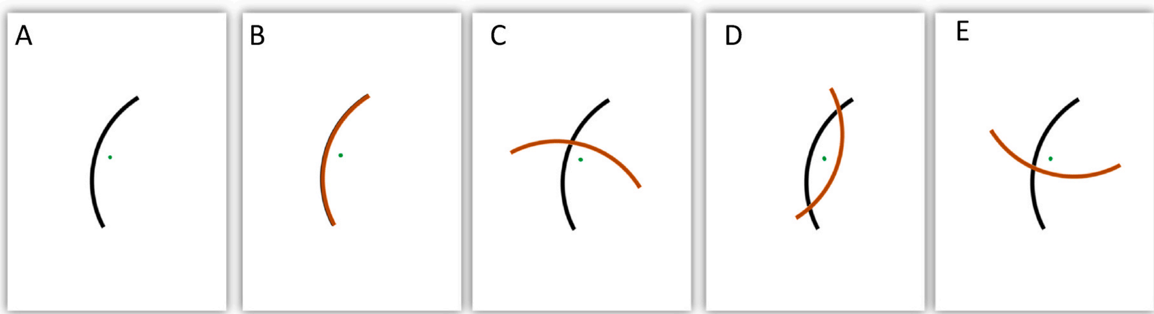

Fig. 7. A. Illustration of an arc stimulus used in Experiment 6, and of its' centroid (green dot), which was not shown during the experiment. B-E. Illustration of Davida's different types of responses when asked to trace the depicted shape with ink (in red ink). (For interpretation of the references to color in this figure legend, the reader is referred to the Web version of this article.)

these shapes' axis of symmetry: a reflection of a shape across its axis of symmetry is, by definition, undetectable, and a reflection of the shape across an axis perpendicular to the axis of symmetry crossing it at the centroid would be indistinguishable from its 180° rotation. Experiment 7 was designed to confirm this hypothesis.

3.3.4. Experiment 7. semicircular arrows

In this experiment, we probed Davida's perception of almost-symmetrical stimuli (a semi-circular arrow) which, unlike completely symmetrical stimuli, would allow detection of reflection errors across a shape-based symmetry axis and across its perpendicular by the centroid, if there are any. In each trial of this experiment, Davida was presented with a semi-circular arrow (diameter: 415 pixels; 6.7 degrees of visual angle; see Fig. 8) for as long as needed and asked to use the computer mouse to move a small round cursor and click as precisely as possible on the tip of the arrow. The arrow was displayed 5 times in each of 12 different orientations: 25 (Fig. 8 A), 55, 85, 115, 145, 175, 205, 235, 265, 295, 325 and 355° clockwise from the vertical. Davida clicked at less than 1 degree of visual angle (62 pixels) from the tip of the arrow in 3.3.% of the trials. In most of the other trials she made 7 types of errors,

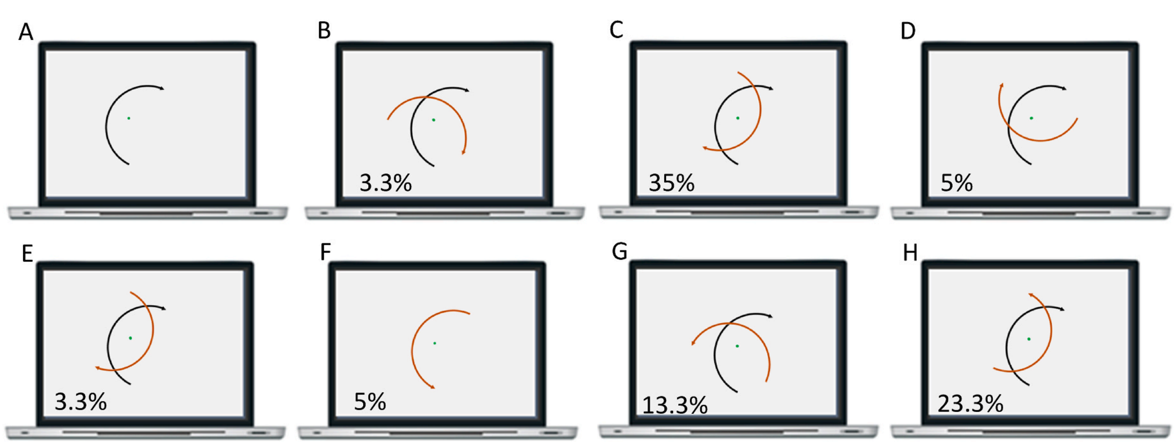

Fig. 8. A. Illustration of a semicircular arrow stimulus used in Experiment 7 and of its centroid (green dot). The green dot was not presented during the experiment. B–H. The tips of semicircular arrows in red ink represent the 7 places in which Davida typically reported perceiving the tip of the depicted stimulus (the arrow shown here in black ink). The percentages correspond to the proportion of trials in which Davida clicked at less than one degree of visual angle from the place where the tip of the arrow in red ink is depicted in each figure. (For interpretation of the references to color in this figure legend, the reader is referred to the Web version of this article.)

consisting in clicking at less than 1 degree of visual angle from the place where the tip of the arrow would have been if the arrow were rotated by 90 (Figs. 8B), 180 (Fig. 8C) or 270 (Fig. 8D) degrees around the shapes' centroid, if it were reflected across the shapes' axis of symmetry (Fig. 8 F) or across an axis perpendicular to the shape's axis of symmetry crossing it at the level of the centroid (Fig. 8 H), or combinations of these errors (Fig. 8, G). In the remaining 5 trials she clicked at a point more than 1 degree of visual angle away from any interpretable landmark. This error profile confirmed that this type of shape is represented with respect to a reference frame aligned with the shape's axis of symmetry and centered on the shape's centroid.

3.4. Experiment 8–9. The reference frame of elongated symmetrical shapes

That both the center of the longest part of an asymmetrical elongated shape and the centroid of a symmetrical shape devoid of a straight part may be used by the brain to locate the center of reference frames at the level of the ISCRs immediately raises the question of the hierarchy between the two locations when both are available. To address this issue, we first reanalyzed Davida's responses in a previously reported experiment (Vannuscorps et al., 2020) in which she was asked to localize the tip of a large black arrow. This analysis indicated that the center of the frame was located at the center of the longest segment rather than on the centroid of this type of shape. This conclusion was confirmed in Experiment 9, which tested Davida's perception of the orientation of two distinct arrows of the same length characterized by very different centroids.

3.4.1. Experiment 8. large arrow

Here, we re-analyzed Davida's responses to 560 trials in an experiment in which she was asked to localize the tip of a large ($\pm10 \times 6$ degrees of visual angle) black arrow pointing left, right, up or down displayed at the center of a computer screen for an unlimited duration. On each trial, Davida was asked to use the computer mouse to move a small round cursor and click as precisely as possible on the tip of the arrow.

We calculated the distance between the coordinates of Davida's response (where she reported seeing the tip of the arrow) and the place where the tip of the arrow would have been if the center of the representational frame was the center of the long axis (Fig. 9 A, red dot) or the shape's centroid (Fig. 9A, green dot). As shown in Fig. 9B–E, she typically located the tip of the arrow (the correct location is illustrated by the black triangle in Fig. 9B–E) closer on average to where it would have been if the arrow were rotated by 90, 180 or 270° around the center of the long axis (illustrated by the red dot in Fig. 9B–E; 38 pixels; SD = 21; 6 mm), than to where it would have been if the center of the representational frame was the arrow's centroid (illustrated by the green dot; 94 pixels; SD = 24; 15 mm). The result of a paired sample *t*-test indicated that this difference is significant ($t\,(559) = 24.8$, $p < 0.001$, $d = 1.05$). A very similar profile emerged when only the first or second half of the items were considered in the analysis (first half: $t\,(279) = 15.7$; second half: $t\,(279) = 19.6$), suggesting that this response profile was reliable throughout the experiment. This suggests that, at least at the level of the ISCRs, the visual system locates the reference frame at the center of the shape's longest segment rather than on the shape's centroid when both are available.

3.4.2. Experiment 9. large and thin arrows

In this experiment, a long arrow with a narrow head ($\pm9.7 \times 6$ degrees of visual angle) and a long arrow with a large head ($\pm9.7 \times 2.8$ degrees of visual angle), both pointing towards the right of the screen, were displayed for an unlimited duration three times at each of 8 different locations on the screen (1.6 or 3.2 degree of visual angle above and on the left, above and on the right, below and on the left or below and on the right of the center of the screen), for a total of 48 trials (2 arrows x 8 orientations x 3 repetitions). In each trial, Davida was asked to use the computer mouse to move a small round cursor and click as precisely as possible on the tip of the arrow. The Movie S2, online, is a recording of Davida performing this task and illustrates her response profile.

As in Experiment 8, we calculated the distance between the coordinates of Davida's response in each trial and the place where the tip of the arrow would have been if the center of the representational frame were the center of the long axis (Fig. 10, red dots) or the shape's centroid (Fig. 10, green dot). In the 24 trials with the arrow composed of a narrow head, Davida located the position of the tip of the arrow accurately (i.e., she clicked at less than 100 pixels from the accurate position of the tip) in 2 trials. In the other trials, she always mislocated the position of the tip to approximately (i.e., less than 100 pixels) where it would have been if the arrow had been rotated by 90° (16%), 180° (50%) or 270° (21%) around the center of the arrow's longest segment (average distance = 35 pixels, SD = 26). All but two of Davida's errors fell closer to where the tip would have been if it were rotated around the center than around the centroid. The results of a paired samples *t*-test indicated that she located the tip of the arrow significantly closer to where the tip would have been if it were rotated around the center than around the centroid ($t\,(21) = 4.7$, $p < 0.001$, $d = 1$).

In the 24 trials with the arrow composed of a large head, Davida located the position of the tip of the arrow accurately (i.e., she clicked at less than 100 pixels from the accurate position of the tip) in 4 trials (17%) and mislocated the position of the tip to approximately (i.e., less

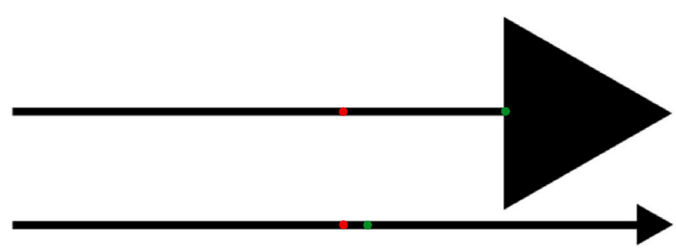

Fig. 10. Illustration of the stimuli used in Experiment 9, of the center of their longest segment (red dot) and of their centroid (green dot). (For interpretation of the references to color in this figure legend, the reader is referred to the Web version of this article.)

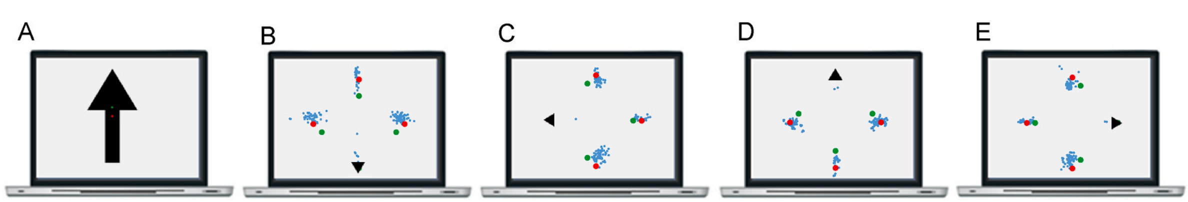

Fig. 9. A. Illustration of the center of the arrow's long axis (red dot) and of the arrow's centroid (green dot). B-E. Each blue dot represents the coordinates of one attempt of Davida to localize the tip (illustrated by the tip of the black triangle) of an arrow pointing down (B), left (C), up (D) or right (E). The red and green dots illustrate where the tip of the arrow would have been if the center of the representational frame were the center of the long axis (red) or of the arrow's centroid (green). (For interpretation of the references to color in this figure legend, the reader is referred to the Web version of this article.)

than 100 pixels) where it would have been if the arrow had been rotated by 180° (71%) or 270° (12.5%) around the center of the arrow's longest segment (average distance = 24 pixels, SD = 18). All of Davida's errors fell closer to where the tip would have been if it were rotated around the center than around the centroid. The results of a paired samples *t*-test indicated that she located the tip of the arrow significantly closer to where the tip would have been if it were rotated around the center than around the centroid (t (18) = 14.8, $p < 0.001$, $d = 3.4$).

4. Discussion

Visual perception results from multiple stages of processing. A major goal of vision science is to characterize the form that mental representations take along these stages. Accordingly, a very large number of studies using a range of different approaches (computational, psychophysical, behavioral, physiological, neuropsychological) have been devoted to this issue. As a result, it has now become clear that vision starts with a representation of some type(s) of visual primitive(s) coded in a retinocentric frame and ends up with representations of objects (cars, dogs, cups) in various (e.g., body-centered, spatiotopic, attentional) non-retinocentric frames. In contrast, we still know very little about the nature of representational units and reference frames at intermediate stages of processing.

The features of Davida's highly selective visual disorder, summarized in the introduction (see also Vannuscorps et al., 2020), suggest that an intermediate stage of processing in the visual system represents bounded areas of the visual field in a reference frame composed of orthogonal axes, aligned with and centered on geometrical properties of the shape itself (e.g., on the elongation axis of elongated shapes). We refer to the type of representation at this level of processing as "intermediate shape-centered representation" (ISCRs). The goal of the nine experiments reported in this article was to use Davida's pattern of errors as a tool for specifying in greater detail the geometrical properties of the reference frame used to represent elongated shapes (Experiments 1–3) and for exploring the properties of the reference frame for symmetrical shapes lacking a straight segment (Experiments 4–7) and for symmetrical shapes composed of a long straight segment (Experiment 8–9).

In Experiment 1–3, we tested Davida's perception of asymmetrical elongated shapes. Virtually all of her responses took the form of a reflection of the shapes across an axis aligned precisely with their longest segment, of a reflection across an axis perpendicular to their longest segment and crossing it at its center, of rotations of the shape around the center of the longest segment, and of combinations of these errors. In Experiments 4–7, we tested Davida's perception of (almost) symmetrical shapes deprived of a straight segment. All of Davida's errors could be characterized as a rotation of the shape across an origin located at its centroid, a reflection of the shape across its axis of symmetry, a reflection of the shape across an axis perpendicular to its axis of symmetry and crossing it at the level of its centroid, and combinations of these errors. These findings suggest that ISCRs are represented in reference frames composed of orthogonal axes aligned with and centered onto the most elongated segment of elongated shapes and, for symmetrical shapes deprived of a straight segment, aligned with their axis of symmetry, and centered on their centroid.

This led to the question of whether the visual system uses the center or the centroid, when both are available, to locate the reference frame of an ISCR. The results in Experiments 8 and 9 suggest that, at the level of the ISCRs, the brain locates the center of the reference frame of symmetrical shapes composed of a straight segment at the center of the longest segment of the shape rather than at its centroid.

The hypothesis that at one or several stage(s) of processing the visual system computes "objects" with respect to their own reference frame is not new and has received support from both neuropsychological and neurophysiological studies (Caramazza and Hillis, 1990; Driver et al., 1994; Marr and Nishihara, 1978; Olson, 2003; Tipper and Behrmann, 1996). Neurophysiological recording studies in monkeys have shown that some neurons in the supplementary eye field respond selectively to particular locations within a reference object (Olson, 2003); and that some ventral-temporal object-responsive areas compute representations of objects that are independent of their position, size and orientation in retinal coordinates (Logothetis et al., 1995; Pasupathy and Connor, 2001; Rollenhagen and Olson, 2000). For instance, a neuron in V4d may respond preferentially to shapes that contain a sharp convexity on the left independently of the retinotopic size and location of that shape (El-Shamayleh and Pasupathy, 2016; Pasupathy and Connor, 2001). Neuropsychological studies have reported brain-damaged patients who suffered from disorders affecting only or disproportionately one half of a stimulus independently of its body-centered location or orientation (Almeida et al., 2020; Caramazza and Hillis, 1990a; Driver et al., 1994; Gainotti et al., 1972; Driver and Halligan, 1991; Tipper and Behrmann, 1996). Such disorders would be difficult to explain without invoking the existence of some type of "object"-centered representation. However, the different construals of "object" in these studies, the corresponding stages of processing in the visual system and the exact properties that determine the center and orientation of the reference frame have remained largely underspecified. In contrast, the results reported in this study invite clear hypotheses about the representational content and reference frame at one precise stage of processing within the visual system – the ISCR.

In a previous study, we proposed that the ISCRs are computed at an early stage of processing, common (and thus preliminary) to the different types of "higher" representational frames (spatiotopic, attentional, body-centered) and to the main functional divisions (perception, recognition, action) that characterize high-level vision (Vannuscorps et al., 2020). This conclusion was supported by Davida's highly consistent proportion and type of errors in all the visual tasks that we used with her, including (speeded) action tasks that are widely assumed to rely on body-centered representations computed in the visual dorsal stream. Under this hypothesis, the findings reported here are relevant, and have the potential to guide future research and theories spanning the cognitive and neural bases of visual perception, object recognition and visuo-motor interactions (e.g., Connor and Knierim, 2017; Marr and Nishihara, 1978; Milner and Goodale, 2006; Riesenhuber and Poggio, 2000). Beyond this implication for fundamental research in vision science, our findings also suggest new directions in the design of intermediate layers for future biologically-inspired artificial neural networks aiming to reproduce aspects of human perception and action.

Whether the principles identified by studying Davida's errors may also determine how reference frames are specified at other stages of processing or whether the nature of reference frames varies across stages of processing within the visual system is a matter for future research. For example, neuropsychological studies of patients suffering from "object-" centered hemineglect would be very useful for informing this question (Driver and Halligan, 1991). If the principles that determine the origin and orientation of reference frames at the level of the ISCRs also apply at other levels of shape representation, one should expect the dividing line between the neglected and spared sides of stimuli to correspond to the characteristics of the reference frames revealed by Davida's profile of rotation and reflection errors.

In line with this possibility, available evidence seems to indicate that the geometrical cues used to assign reference frames at the stage of the ISCRs may apply more broadly. Indeed, a number of previous studies have proposed that a shape's axis of elongation and axis of symmetry may be particularly salient (Quinlan and Humphreys, 1993; Sekuler and Swimmer, 2000), may play a role in the computation of orientation-invariant shape representations subserving recognition (Leek and Johnston, 2006; Ling and Sanocki, 1995; Quinlan and Humphreys, 1993; Tarr and Pinker, 1990) and/or underpin the perception of the orientation of shapes (Boutsen and Marendaz, 2001; Cohen and Singh, 2006; Gregory and McCloskey, 2010; McCloskey et al., 2006). Quilan and Humphreys (1993), for instance, found that participants asked to draw what they considered to be the most salient axis of a series of shapes (a line that they felt most naturally belonged in the shape) almost always drew the axis of symmetry if the shape possessed one. Leek and Johnston (2006) showed that the time required to recognize a previously memorized abstract shape is less affected by the orientation of the test stimulus when the shape has a salient axis of symmetry. Chaisilprungraung et al. (2019) showed, based on an analysis of healthy participant's reflection errors in a visual memory task, that asymmetrical elongated shapes are represented in reference frames aligned precisely with the shape's longest segment. In each trial of that study, two pictures of an asymmetrical elongated object (e.g., a hammer, a hatchet) were presented in turn for 750 ms at a random orientation. Participants were asked to memorize the orientation of both objects and, then, to use the computer keyboard (to change the tilt) and the mouse (to flip the image) to reproduce their orientation as precisely as possible. In line with our findings with Davida, the analysis of the participants' errors indicated that reflections occurred across axes aligned either with the shape's longest segment or with its perpendicular. Although the level of representation probed in these studies is not totally clear, the findings suggest that the heuristics that determine the location (origin) and orientation of reference frames at the stage of the ISCRs may apply to the representation of shapes and objects more broadly within the visual and cognitive system.

Other behavioral and functional neuroimaging studies have provided evidence that shapes may also be represented with respect to a type of skeletal representation computed from a family of medial axis transformations of the shape (Ayzenberg and Lourenco, 2019; Blum, 1967; Feldman and Singh, 2006; Firestone and Scholl, 2014; Harrison and Feldman, 2009; Hung et al., 2012; Kimia, 2003; Kovács et al., 1998; Lescroart and Biederman, 2013; Lowet et al., 2018). The medial axis transformation of most shapes, including those used in the experiments reported here, does not include any representation of the shapes' "center" or centroid, and it does not include any axis perpendicular to the shapes' main axis. Therefore, it is unclear how medial axis representations could account for Davida's pattern of errors.

Nevertheless, our data should not be taken as an argument against the existence of medial axis representations. It is possible, perhaps likely, that medial axis representations and orthogonal shape-centered reference frames co-exist to support different computational goals. Orthogonal shape-centered reference frames are very easy to compute. By definition, they are composed of perpendicular axes made of straight lines. Hence, assigning such reference frame to a shape requires only determining where to locate its center and how to orient one of its axis which, as shown here, may be achieved based on salient properties of the to-be-represented shapes. Despite this simplicity, representing shapes in their own coordinate system provides a computationally efficient way to represent their location and orientation, first with respect to their initial retinocentric representation, and then to different behaviorally-relevant attentional, body-centered or spatiotopic reference frames, with just a few parameters (McCloskey et al., 2006).

A weakness of shape-centered representations within orthogonal reference frames, however, is that they are severely influenced by transformations that change the objective shape of objects (such as rotations in depth, stretching, bending or shearing), making them suboptimal to support object recognition. In contrast, some medial axis transformations (e.g., pruned medial axis models and models based on a Bayesian estimation of the most likely generative skeleton) appear to be relatively insensitive to such transformations (Blum, 1967; Kimia, 2003; Ayzenberg and Lourenco, 2019). Hence, medial axis representations could play a role in a stage of visual processing subsequent to that of the ISCRs and specialized in the representation of shapes for their recognition. In line with this proposal, the medial axis has been shown to constitute a basis of shape categorization and perceptual similarity judgments (Ayzenberg and Lourenco, 2019; Lowet et al., 2018) and the representation of the medial axis structure of three-dimensional objects has been identified in the inferior temporal (IT) cortex (Lescroart and Biederman, 2013).

Although the findings reported in this study provide new insights into the heuristics used by the visual system to locate and orient reference frames at the level of the ISCRs, our conclusions are drawn from, and therefore limited to, a very small sample of possible shapes. The extent to which our findings generalize to other types of elongated and symmetrical shapes will need to be explored in future studies. It is possible, for instance, that the location of the center of symmetrical elongated shapes may depends on the saliency of the shape's symmetry and elongation axes (Sekuler and Swimmer, 2000). In Quinlan and Humphreys' (1993) study, for instance, the tendency of participants to draw a shape's axis in line with their axis of symmetry or their axis of elongation depended on the saliency of the shape's axis of elongation. Likewise, future studies will be needed to determine the nature of the reference frame used to represent other types of shapes, such as asymmetrical elongated curved shapes and surfaces, shapes deprived of any salient axis, shapes that have more than a salient axis, and shapes whose axis of symmetry and elongation are not confounded.

Author statement

Alfonso Caramazza: Supervision, Funding, Conceptualization; Writing - Review and Editing. **Albert Galaburda**: Conceptualization, Writing - Review and Editing. **Gilles Vannuscorps:** Conceptualization, Methodology, Validation, Analysis, Investigation, Writing - Original Draft, Review and Editing, Data Curation.

Declaration of competing interest

The authors declare no competing interests.

Acknowledgments

We are grateful to Davida and her family for their time, motivation, and kindness. This research was supported by the Mind, Brain and Behavior Interfaculty Initiative provostial funds to A.C.

References

Almeida, J., Freixo, A., Tábuas-Pereira, M., Herald, S.B., Valério, D., Schu, G., Santana, I., 2020. Face-specific perceptual distortions reveal A view- and orientation-independent face template. Curr. Biol. 30 (20) https://doi.org/10.1016/j.cub.2020.07.067.

Arguin, M., Marleau, I., Aubin, M., Zahabi, S., Leek, E.C., 2019. A surface-based code contributes to visual shape perception. J. Vis. 19 (11) https://doi.org/10.1167/19.11.6.

Ayzenberg, V., Lourenco, S.F., 2019. Skeletal descriptions of shape provide unique perceptual information for object recognition. Sci. Rep. 9 (1) https://doi.org/10.1038/s41598-019-45268-y.

Barton, J.J.S., Malcolm, G.L., Hefter, R.L., 2007. Spatial processing in Bálint syndrome and prosopagnosia: a study of three patients. J. Neuro Ophthalmol. 27 (4) https://doi.org/10.1097/WNO.0b013e31815b9b85.

Baylis, G.C., Baylis, L.L., Gore, C.L., 2004. Visual neglect can be object-based or scene-based depending on task representation. Cortex 40 (2). https://doi.org/10.1016/S0010-9452(08)70119-9.

Beschin, N., Cubelli, R., Della Sala, S., Spinazzola, L., 1997. Left of what? The role of egocentric coordinates in neglect. J. Neurol. Neurosurg. Psychiatry 63 (4). https://doi.org/10.1136/jnnp.63.4.483.

Bisiach, E., Capitani, E., Porta, E., 1985. Two basic properties of space representation in the brain: evidence from unilateral neglect. J. Neurol. Neurosurg. Psychiatry 48 (2). https://doi.org/10.1136/jnnp.48.2.141.

Blum, H., 1967. MIT press. In: A Transformation for Extracting New Descriptors of Shape. MIT press, Cambridge.

Boutsen, L., Marendaz, C., 2001. Detection of shape orientation depends on salient axes of symmetry and elongation: evidence from visual search. Percept. Psychophys. 63 (3) https://doi.org/10.3758/BF03194408.

Bryant, B.R., Wiederholt, J.L., Bryant, D.P., 1991. Gray Diagnostic Reading Tests–, second ed. Pro-, Austin, TX (GRDT-2).

Calvanio, R., Petrone, P.N., Levine, D.N., 1987. Left visual spatial neglect is both environment-centered and body-centered. Neurology 37 (7). https://doi.org/10.1212/wnl.37.7.1179.

Caramazza, A., Hillis, A.E., 1990a. Levels of representation, co-ordinate frames, and unilateral neglect. Cogn. Neuropsychol. 7 (5–6), 391–445.

Caramazza, A., Hillis, A.E., 1990b. Spatial representation of words in the brain implied by studies of a unilateral neglect patient. Nature 346 (6281), 267–269. https://doi.org/10.1038/346267a0.

Chaisilprungraung, T., German, J., McCloskey, M., 2019. How are object shape axes defined? Evidence from mirror-image confusions. J. Exp. Psychol. Hum. Percept. Perform. 45 (1), 111.

Cheng, K., 2005. Reflections on geometry and navigation. Connect. Sci. 17 (1–2) https://doi.org/10.1080/09540090500138077.

Cohen, E.H., Singh, M., 2006. Perceived orientation of complex shape reflects graded part decomposition. J. Vis. 6 (8) https://doi.org/10.1167/6.8.4.

Colby, C.L., 1998. Action-oriented spatial reference frames in cortex. Neuron 20 (1), 15–24. https://doi.org/10.1016/S0896-6273(00)80429-8.

Conners, C.K., 2010. Conners Comprehensive Behavior Rating Scales (Conners CBRS) (Multi-Health Systems).

Connor, C.E., Knierim, J.J., 2017. Integration of objects and space in perception and memory. Nat. Neurosci. 20 (11), 1493–1503.

De Valois, R.L., De Valois, K.K., 1988. In: Press, O.U. (Ed.), Spatial Vision (New-York).

Delis, D.C., Kaplan, E., Kramer, J.H., 2001. Delis-kaplan executive function System®(D-KEFS®): examiner's manual: flexibility of thinking, concept formation. Prob. Solving Plan. Creativ. Impluse Cont. Inhibition Person.

Driver, J., Halligan, P.W., 1991. Can visual neglect operate in object-centred Co-ordinates? An affirmative single-case study. Cogn. Neuropsychol. 8 (6), 475–496. https://doi.org/10.1080/02643299108253384.

Driver, J., Baylis, G.C., Goodrich, S.J., Rafal, R.D., 1994. Axis-based neglect of visual shapes. Neuropsychologia 32 (11), 1353–1356. https://doi.org/10.1016/0028-3932(94)00068-9.

El-Shamayleh, Y., Pasupathy, A., 2016. Contour curvature as an invariant code for objects in visual area V4. J. Neurosci. 36 (20), 5532–5543. https://doi.org/10.1523/JNEUROSCI.4139-15.2016.

Farah, M.J., Brunn, J.L., Wong, A.B., Wallace, M.A., Carpenter, P.A., 1990. Frames of reference for allocating attention to space: evidence from the neglect syndrome. Neuropsychologia 28 (4). https://doi.org/10.1016/0028-3932(90)90060-2.

Feldman, J., Singh, M., 2006. Bayesian estimation of the shape skeleton. Proc. Natl. Acad. Sci. U. S. A 103 (47). https://doi.org/10.1073/pnas.0608811103.

Firestone, C., Scholl, B.J., 2014. "Please tap the shape, anywhere you like": shape skeletons in human vision revealed by an exceedingly simple measure. Psychol. Sci. 25 (2) https://doi.org/10.1177/0956797613507584.

Gainotti, G., Messerli, P., Tissot, R., 1972. Qualitative analysis of unilateral spatial neglect in relation to laterality of cerebral lesions. J. Neurol. Neurosurg. Psychiatr. 35 (4), 545–550. https://doi.org/10.1136/jnnp.35.4.545.

Gioia, G.A., Isquith, P.K., Guy, S.C., Kenworthy, L., 2000. BRIEF: Behavior rating inventory of executive function. Psychol. Assess. Resour.

Gregory, E., McCloskey, M., 2010. Mirror-image confusions: implications for representation and processing of object orientation. Cognition 116 (1), 110–129. https://doi.org/10.1016/j.cognition.2010.04.005.

Harrison, S.J., Feldman, J., 2009. The influence of shape and skeletal axis structure on texture perception. J. Vis. 9 (6) https://doi.org/10.1167/9.6.13.

Hillis, A.E., Caramazza, A., 1995. A framework for interpreting distinct patterns of hemispatial neglect. Neurocase 1 (3). https://doi.org/10.1080/13554799508402364.

Hillis, A.E., Rapp, B., Benzing, L., Caramazza, A., 1998. Dissociable coordinate frames of unilateral spatial neglect: "Viewer- centered" neglect. Brain Cognit. 37 (3) https://doi.org/10.1006/brcg.1998.1010.

Horton, J.C., Hoyt, W.F., 1991a. Quadrantic visual field defects: a hallmark of lesions in extrastriate (v2/v3) cortex. Brain 114 (4). https://doi.org/10.1093/brain/114.4.1703.

Horton, J.C., Hoyt, W.F., 1991b. The representation of the visual field in human striate cortex: a revision of the classic holmes map. Arch. Ophthalmol. 109 (6) https://doi.org/10.1001/archopht.1991.01080060080030.

Hubel, D.H., Wiesel, T.N., 1968. Receptive fields and functional architecture of monkey striate cortex. J. Physiol. 195 (1) https://doi.org/10.1113/jphysiol.1968.sp008455.

Hummel, J.E., 2001. Complementary solutions to the binding problem in vision: implications for shape perception and object recognition. Vis. Cognit. 8 (3–5) https://doi.org/10.1080/13506280143000214.

Hung, C.C., Carlson, E.T., Connor, C.E., 2012. Medial Axis shape coding in macaque inferotemporal cortex. Neuron 74 (6). https://doi.org/10.1016/j.neuron.2012.04.029.

Karnath, H.O., Schenkel, P., Fischer, B., 1991. Trunk orientation as the determining factor of the "contralateral" deficit in the neglect syndrome and as the physical anchor of the internal representation of body orientation in space. Brain 114 (4). https://doi.org/10.1093/brain/114.4.1997.

Kimia, B.B., 2003. On the role of medial geometry in human vision. J. Physiol. Paris 97. https://doi.org/10.1016/j.jphysparis.2003.09.003.

Kovács, I., Fehér, Á., Julesz, B., 1998. Medial-point description of shape: a representation for action coding and its psychophysical correlates. Vis. Res. 38 (15–16) https://doi.org/10.1016/S0042-6989(97)00321-0.

Ladavas, E., 1987. Is the hemispatial deficit produced by right parietal lobe damage associated with retinal or gravitational coordinates? Brain 110 (1). https://doi.org/10.1093/brain/110.1.167.

Leek, E.C., Johnston, S.J., 2006. A polarity effect in misoriented object recognition: the role of polar features in the computation of orientation-invariant shape representations. Vis. Cognit. 13 (5) https://doi.org/10.1080/13506280544000048.

Leek, E.C., Reppa, I., Arguin, M., 2005. The structure of three-dimensional object representations in human vision: evidence from whole-part matching. J. Exp. Psychol. Hum. Percept. Perform. 31 (4) https://doi.org/10.1037/0096-1523.31.4.668.

Lescroart, M.D., Biederman, I., 2013. Cortical representation of medial axis structure. Cerebr. Cortex 23 (3). https://doi.org/10.1093/cercor/bhs046.

Ling, X., Sanocki, T., 1995. Major axes as a moderately abstract model for object recognition. Psychol. Sci. 6 (6) https://doi.org/10.1111/j.1467-9280.1995.tb00528.x.

Logothetis, N.K., Pauls, J., Poggio, T., 1995. Shape representation in the inferior temporal cortex of monkeys. Curr. Biol.: CB 5 (5), 552–563. Retrieved from. http://www.ncbi.nlm.nih.gov/pubmed/7583105.

Lowet, A.S., Firestone, C., Scholl, B.J., 2018. Seeing structure: shape skeletons modulate perceived similarity. Atten. Percept. Psychophys. 80 (5) https://doi.org/10.3758/s13414-017-1457-8.

Marr, D., 1982. Vision: a computational investigation into the human representation and processing of visual information. Vision: Comput. Invest. Into Human Represent. Process Visual Inform. https://doi.org/10.1016/0022-2496(83)90030-5.

Marr, D., Nishihara, H.K., 1978. Representation and recognition of the spatial organization of three-dimensional shapes. Proc. Roy. Soc. Lond. B Biol. Sci. 200 (1140), 269–294. https://doi.org/10.1098/rspb.1978.0020.

McCarney, D., Greenberg, L.M., 1990. Test of Variables of Attention (TOVA). Attention Technology, St. Paul.

McCloskey, M., Valtonen, J., Cohen Sherman, J., 2006. Representing orientation: a coordinate-system hypothesis and evidence from developmental deficits. Cogn. Neuropsychol. 23 (5), 680–713. https://doi.org/10.1080/02643290500538356.

McFadzean, R.M., Hadley, D.M., 1997. Homonymous quadrantanopia respecting the horizontal meridian: a feature of striate and extrastriate cortical disease. Neurology 49 (6). https://doi.org/10.1212/WNL.49.6.1741.

Melcher, D., Morrone, M.C., 2015. Nonretinotopic visual processing in the brain. Vis. Neurosci. 32, E017. https://doi.org/10.1017/S095252381500019X.

Milner, D., Goodale, M., 2006. The Visual Brain in Action, 2 ed. Oxford University Press, Oxford. https://doi.org/10.1093/acprof:oso/9780198524724.001.0001.

Mullette-Gillman, O.A., Cohen, Y.E., Groh, J.M., 2005. Eye-centered, head-centered, and complex coding of visual and auditory targets in the intraparietal sulcus. J. Neurophysiol. 94 (4) https://doi.org/10.1152/jn.00021.2005.

Olson, C.R., 2003. Brain representation of object-centered space in monkeys and humans. Annu. Rev. Neurosci. 26 (1), 331–354.

Palmer, S.E., 1985. The role of symmetry in shape perception. Acta Psychol. 59 (1), 67–90. https://doi.org/10.1016/0001-6918(85)90042-3.

Palmer, S.E., 1999. Vision science: photons to phenomenology. In: Bradford Bokk. MIT press.

Palmer, S., Rock, I., 1994a. Rethinking perceptual organization: the role of uniform connectedness. Psychomic Bull. Rev. 1 (1), 29–55. https://doi.org/10.3758/BF03200760.

Palmer, S., Rock, I., 1994b. Rethinking perceptual organization: the role of uniform connectedness. Psychomic Bull. Rev. https://doi.org/10.3758/BF03200760.

Pasupathy, A., Connor, C.E., 2001. Shape representation in area V4: position-specific tuning for boundary conformation. J. Neurophysiol. 86 (5), 2505–2519. https://doi.org/10.1152/jn.2001.86.5.2505.

Peirce, J.W., 2007. PsychoPy—psychophysics software in Python. J. Neurosci. Methods 162 (1–2), 8–13.

Peirce, J.W., 2009. Generating stimuli for neuroscience using PsychoPy. Front. Neuroinf. 2, 10.

Pospisil, D.A., Pasupathy, A., Bair, W., 2018. Artiphysiology'reveals V4-like shape tuning in a deep network trained for image classification. Elife 7, e38242.

Quinlan, P.T., Humphreys, G.W., 1993. Perceptual frames of reference and two-dimensional shape recognition: further examination of internal axes. Perception 22 (11), 1343–1364. https://doi.org/10.1068/p221343.

Riesenhuber, M., Poggio, T., 2000. Models of object recognition. N*at. Neurosci.* 3, 1199–1204. https://doi.org/10.1038/81479.

Rock, I., 1983. The Logic of Perception. MIT Press, Cambridge, MA.

Rock, I., Brosgole, L., 1964. Grouping based on phenomenal proximity. J. Exp. Psychol. 67 (6) https://doi.org/10.1037/h0046557.

Rollenhagen, J.E., Olson, C.R., 2000. Mirror-image confusion in single neurons of the macaque inferotemporal cortex. Science 287 (5457), 1506–1508. https://doi.org/10.1126/science.287.5457.1506.

Schubert, T., McCloskey, M., 2013. Prelexical representations and processes in reading: evidence from acquired dyslexia. Cogn. Neuropsychol. 30 (6) https://doi.org/10.1080/02643294.2014.880677.

Sekuler, A.B., Swimmer, M.B., 2000. Interactions between symmetry and elongation in determining reference frames for object perception. Canadian J. Experiment. Psychol. Revue Canadienne de Psychologie Experimentale 54 (1), 42.

Sheslow, D., Adams, W., 2003. Wide Range Assessment of Memory and Learning, second ed. (WRAML2). Wide Range Inc., Delaware.

Tarr, M.J., Pinker, S., 1990. When does human object recognition use a viewer-centered reference frame? Psychol. Sci. 1 (4) https://doi.org/10.1111/j.1467-9280.1990.tb00209.x.

Tipper, S.P., Behrmann, M., 1996. Object-centered not scene-based visual neglect. J. Exp. Psychol. Hum. Percept. Perform. https://doi.org/10.1037/0096-1523.22.5.1261.

Torgesen, J.K., Wagner, R.K., Rashotte, C.A., 2012. TOWRE-2 Examiner's Manual (Austin, TX: Pro-Ed).

Vannuscorps, G., Galaburda, A., Caramazza, A., 2020. Shape-centered representations of bounded regions of space mediate the transformation of retinotopic representations into conscious perception of objects. BioRxiv. https://doi.org/10.1101/2020.05.29.123901, 2020.05.29.123901.

Vaughn-Blount, K., Watson, S.T., Kokol, A.L., Grizzle, R., Carney, R.N., Rich, S.S., et al., 2011. Wechsler intelligence scale for children. In: Encyclopedia of Child Behavior and Development, fourth ed., pp. 1553–1555. https://doi.org/10.1007/978-0-387-79061-9_3066.

Wagner, R., Torgesen, J., Rashotte, C., Pearson, N.A., 1999. CTOPP-2: Comprehensive Test of Phonological Processing, second ed. (Pro-ed Austin, TX).
Wandell, B.A., Dumoulin, S.O., Brewer, A.A., 2007. Visual field maps in human cortex. Neuron 56 (2), 366–383. https://doi.org/10.1016/j.neuron.2007.10.012.
Wiig, E.H., Semel, E.M., Secord, W., 2003. CELF 5: Clinical Evaluation of Language Fundamentals. Pearson/PsychCorp.
Yamins, D.L., Hong, H., Cadieu, C.F., Solomon, E.A., Seibert, D., DiCarlo, J.J., 2014. Performance-optimized hierarchical models predict neural responses in higher visual cortex. Proc. Natl. Acad. Sci. Unit. States Am. 111 (23), 8619–8624.